

Precision jet measurements and determination of $\alpha_s(M_Z)$ by H1 @ HERA

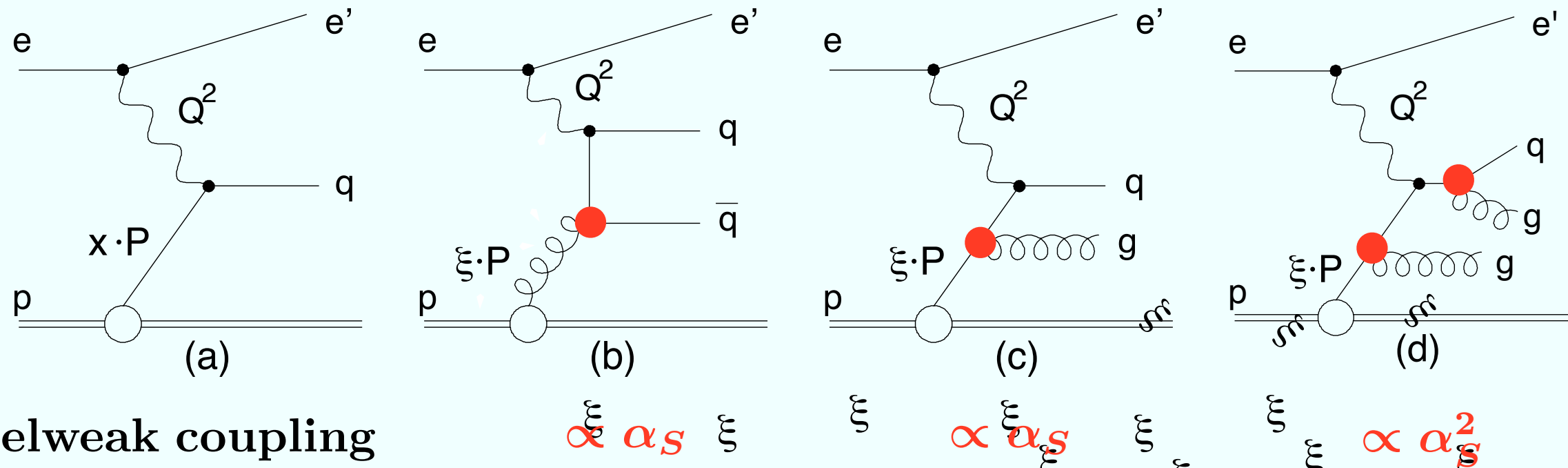
Günter Grindhammer, Max-Planck-Institute for Physics,
on behalf of the H1 collaboration



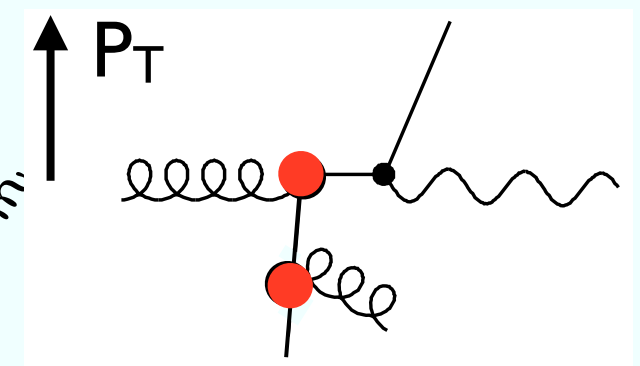
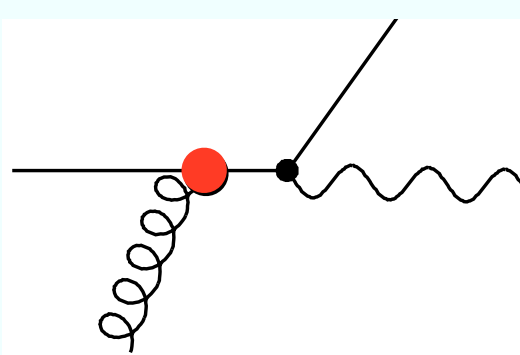
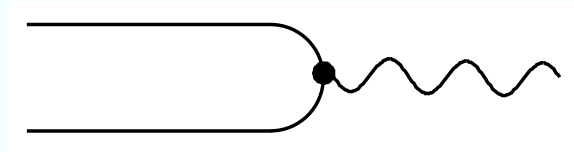
Low-x Meeting, Yukawa Institute, Kyoto, June 17-21, 2014



Multijet production in ep NC DIS



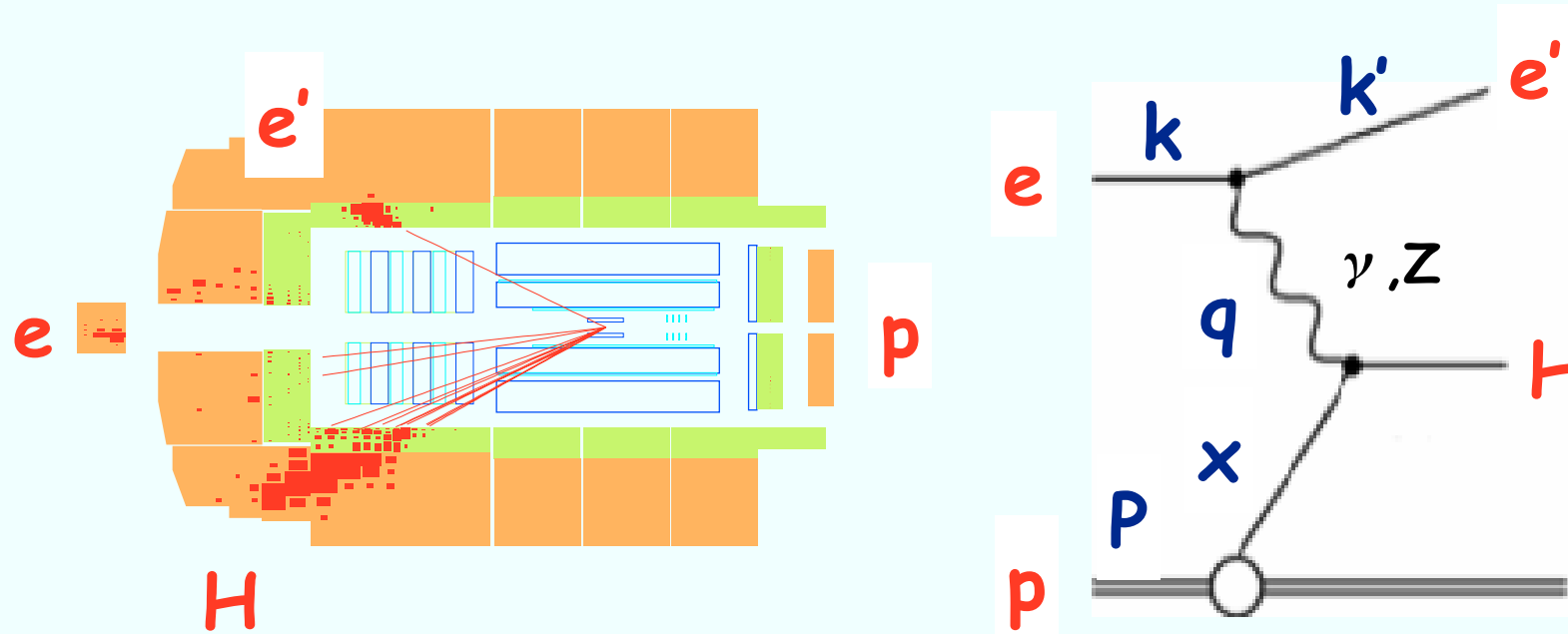
boost events into Breit frame: $2xP + q = 0$



in LO NC DIS depends on q and $q\bar{q}$ densities and only in NLO on alphas (\Rightarrow scaling violations)

jets depend already in LO on $\alpha_s \otimes g (q \text{ or } \bar{q})$ in IS and α_s in FS

NC DIS measurement



virtuality: $Q^2 = -(k - k')^2$
inelasticity: $y = (P \cdot q) / (P \cdot k)$
Bjorken x : $x = Q^2 / (2P \cdot q)$
 $Q^2 = xys$ $s = (k + P)^2$

NC DIS event selection:

- trigger and selection is based on the scattered electron in the LAr cal.
- $150 < Q^2 < 15000 \text{ GeV}^2$
- $0.2 < y < 0.7$

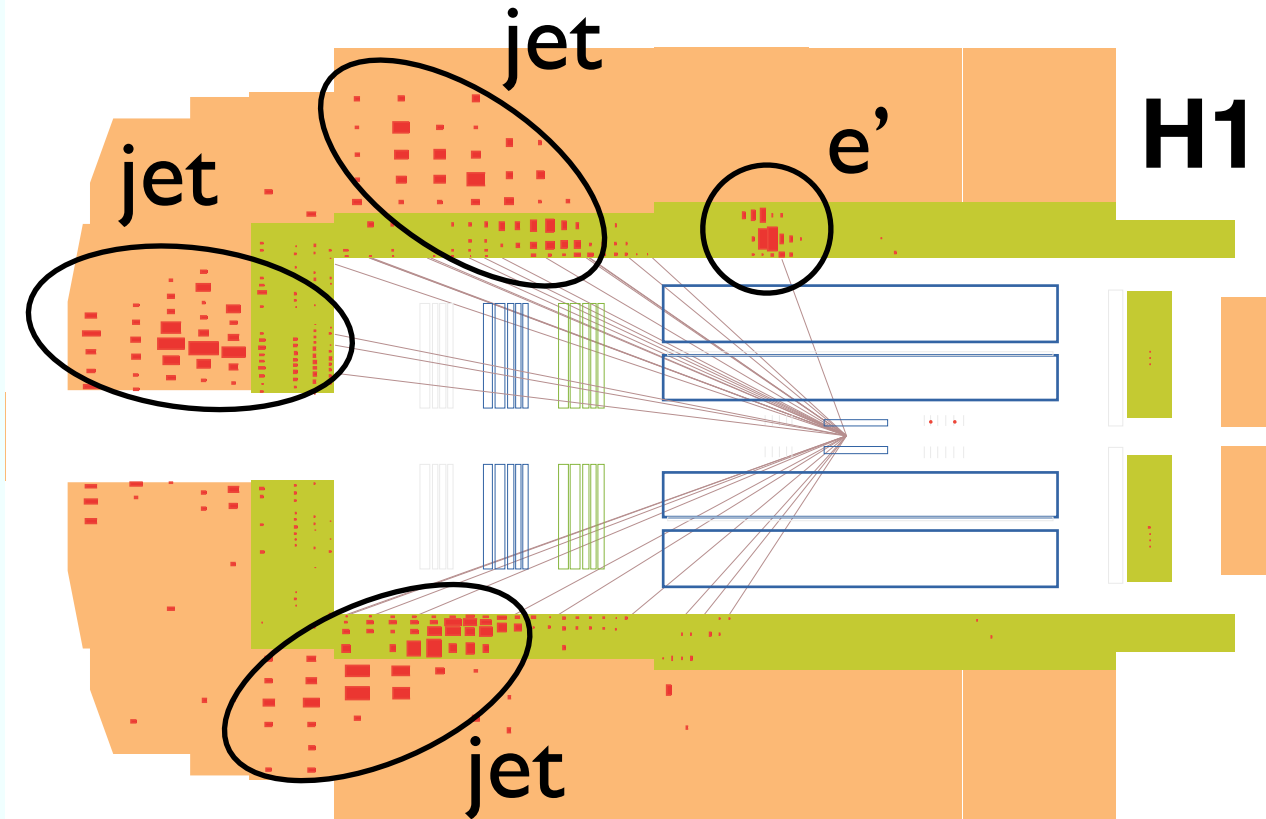
NC measurement \Rightarrow normalized jet cross sections \propto

$N_{\text{jet}}(P_T^{\text{jet}}) / N_{\text{NC}}$ in a given Q^2 bin

$\sigma_{\text{jet}}/\sigma_{\text{NC}}$ benefits from partial cancellation of exp. uncertainties

Multijet measurements

- **Inclusive jets:** every jet in an event, exceeding a minimum P_T contributes to σ_{jet} .
- **Dijets:** events with at least 2 jets above a given P_T contribute to σ_{dijet} .
- **Trijets:** events with at least 3 jets above a given P_T contribute to σ_{trijet} ;



significantly smaller statistics, but high sensitivity to α_s ($O(\alpha_s^2)$ in LO).

- **Kinematic correlations:** are taken into account between the inclusive jets in the inclusive jet sample, between that sample and the dijet and the trijet sample. The trijet events are a subsample of the dijet events.
- **Correlations & detector effects:** may lead to migrations between jet samples and in & out of the measurement phase space.

Observables/Measurements

Reconstruction of jets

- energy flow algorithm:
 - tracks and calorimetric clusters avoiding double counting of energies
 - neural networks to get probability for a cluster to be of em. or had. origin
 - calibration of clusters in jets and outside of jets
- k_T and anti- k_T algorithm in the Breit frame

hadronic energy scale uncertainty
1%

- Inclusive jet: Q^2, P_T^{jet}

$$Q^2, \langle P_T \rangle_2 = \frac{1}{2}(P_T^{\text{jet}1} + P_T^{\text{jet}2})$$

- Dijet:

$$Q^2, \xi_2 = x(1 + M_{12}^2/Q^2)$$

- Trijet:

$$Q^2, \langle P_T \rangle_3 = \frac{1}{3}(P_T^{\text{jet}1} + P_T^{\text{jet}2} + P_T^{\text{jet}3})$$

$$Q^2, \xi_3 = x(1 + M_{123}^2/Q^2)$$

Extended vs. measurement p.s.

	Extended analysis phase space	Measurement phase space for jet cross sections
NC DIS phase space	$100 < Q^2 < 40\,000 \text{ GeV}^2$ $0.08 < y < 0.7$	$150 < Q^2 < 15\,000 \text{ GeV}^2$ $0.2 < y < 0.7$
Jet polar angular range	$-1.5 < \eta_{\text{lab}}^{\text{jet}} < 2.75$	$-1.0 < \eta_{\text{lab}}^{\text{jet}} < 2.5$
Inclusive jets	$P_{\text{T}}^{\text{jet}} > 3 \text{ GeV}$	$7 < P_{\text{T}}^{\text{jet}} < 50 \text{ GeV}$
Dijets and trijets	$3 < P_{\text{T}}^{\text{jet}} < 50 \text{ GeV}$	$5 < P_{\text{T}}^{\text{jet}} < 50 \text{ GeV}$ $M_{12} > 16 \text{ GeV}$

- The extended phase space helps to describe the migrations at the boundaries of the measurement p.s.
- This improves the precision of the jet measurement

Regularized unfolding

$$\vec{m} = A\vec{x}$$

- $\textcolor{red}{m}$... measured detector level distribution
- $\textcolor{red}{A}$... detector response matrix
- $\textcolor{red}{x}$... “true”, i.e. hadron (particle) level distribution

Obtain x by analytical minimization of

TUnfold (S.Schmitt), JINST 7 (2012) T10003,
[arXiv:1205.6201](https://arxiv.org/abs/1205.6201)

$$\chi^2 = (\vec{m} - A\vec{x})^T V_m^{-1} (\vec{m} - A\vec{x}) + \tau^2 (\vec{x} - \vec{x}_0)^T (L^T L) (\vec{x} - \vec{x}_0)$$

V_m is the covariance matrix, the τ^2 term damps fluctuations

All 4 measurements, NC, incl. jets, dijets and trijets
are unfolded simultaneously, yielding most stable results.

Correlations of the data sets are contained in V_m .

Migration matrix

$\vec{\epsilon}$	$\epsilon_{E,-\beta_1,-\beta_2,-\beta_3}$	ϵ_1	ϵ_2	ϵ_3
Detector level	Reconstructed Trijet events which are not generated as Trijet event			Trijet $Q^2, \langle p_T \rangle_3, y,$ Trijet-cuts
	Reconstructed Dijet events which are not generated as Dijet event		Dijet $Q^2, \langle p_T \rangle_2, y,$ Dijet-cuts	
	Reconstructed jets without match to generator level	Incl. Jet $p_T^{\text{jet}}, Q^2, y, \eta$		
	NC DIS Q^2, y			
Hadron level				

Multidimensional unfolding
in Q^2, y, P_T

Migrations taken into account

NC DIS events to preserve the normalization

Detector response from simulations, averaging 2 different MC models

Overall size 4562x1370 bins, about 3% non-zero

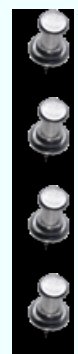
NLO calculations

$$\sigma_{\text{jet}}^{\text{parton}} = \sum_{a,n} \alpha_s^n(\mu_r, \alpha_s(M_Z)) c_{a,n}(x, \mu_r, \mu_f) \otimes f_a(x, \mu_f)$$

LO contribution is of order $O(\alpha_s)$ for inclusive jets & dijet
and of $O(\alpha_s^2)$ for trijet cross sections

The perturbative coefficients $c_{a,n}$ are known in NLO only

The calculations are carried out in the MSbar scheme for 5 active and massless flavors using:



fastNLO framework

NLOjet++ for the coefficients

MSTW2008 PDF set

$\alpha_s(M_Z) = 0.118$

$$\mu_r^2 = \frac{1}{2}(Q^2 + P_T^2) \quad \mu_f^2 = Q^2$$

$$\sigma_{\text{jet}}^{\text{hadron}} = \sigma_{\text{jet}}^{\text{parton}} c^{\text{eweak}} c^{\text{had}}$$

$$\sigma_{\text{jet}}^{\text{hadron}} / \sigma_{\text{NC}} = \sigma_{\text{jet}}^{\text{parton}} c^{\text{had}} / \sigma_{\text{NC}}$$

$$c^{\text{had}} = \sigma^{\text{hadron}} / \sigma^{\text{parton}}$$

$$c^{\text{eweak}} = \sigma^{\gamma,Z} / \sigma^\gamma$$

Jet cross sections measurements

HERA-2 data, 351 pb^{-1}

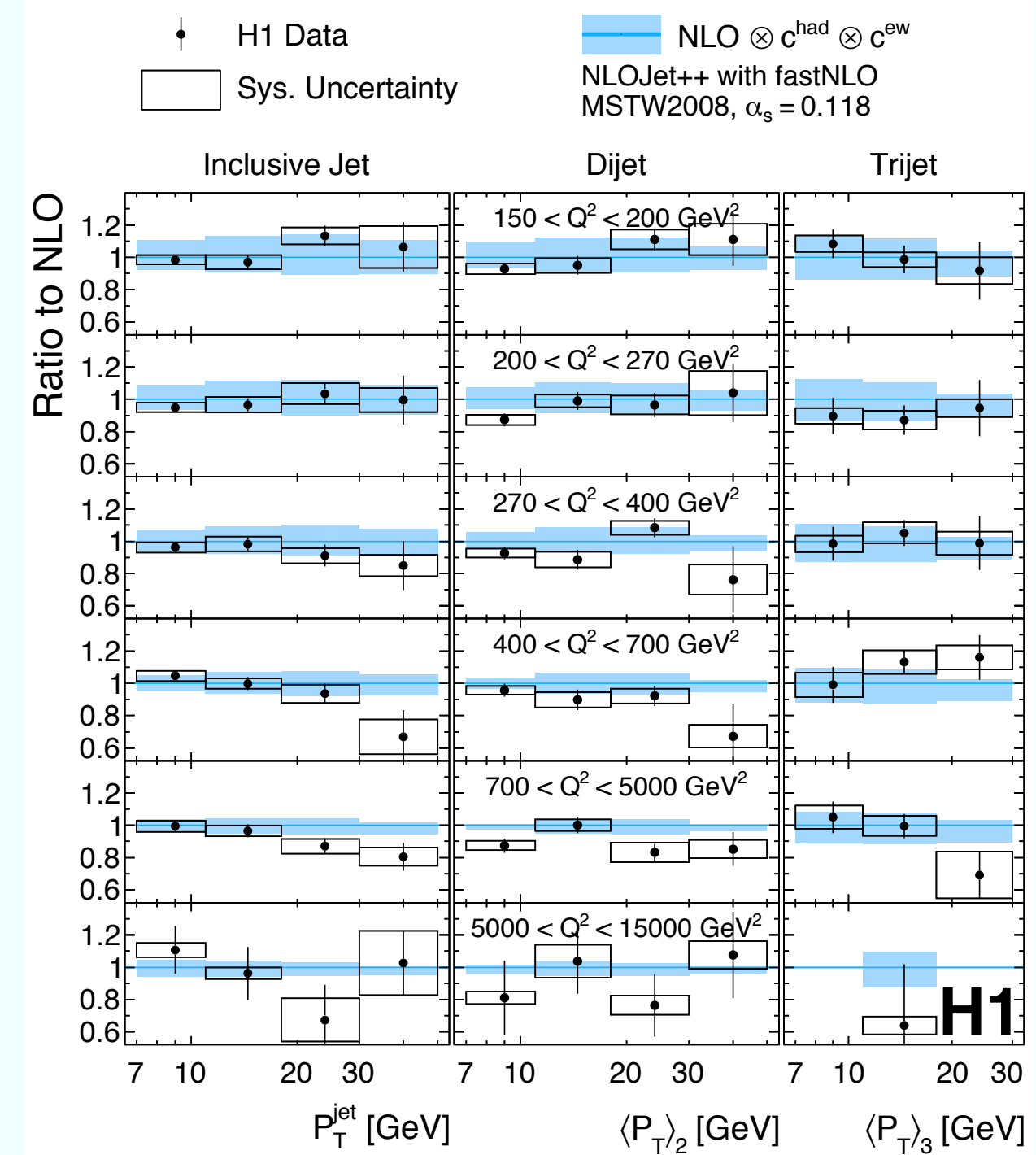
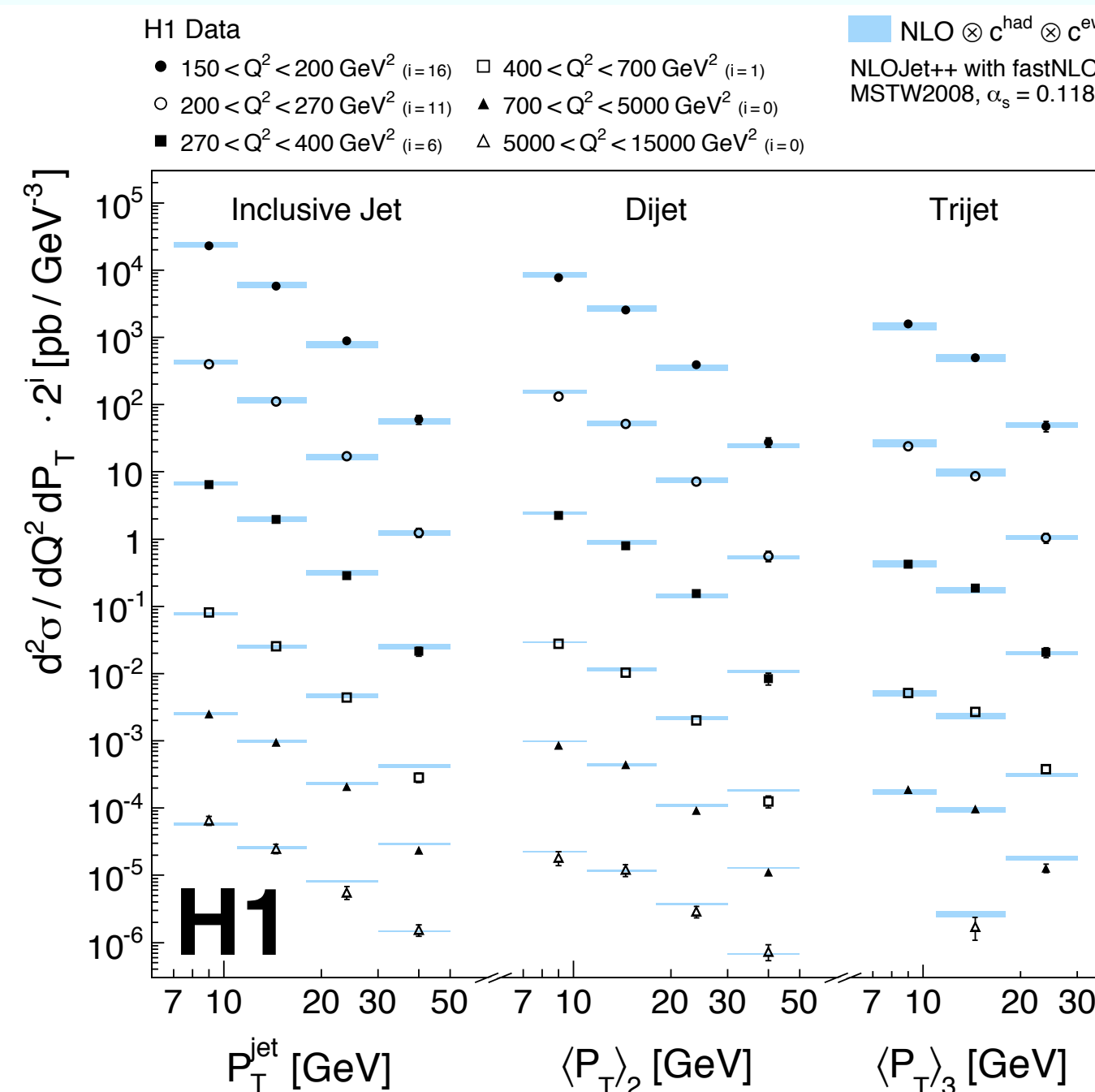
Measurement	NC DIS phase space	Phase space for jet cross sections	
$\sigma_{\text{jet}}(Q^2, P_T^{\text{jet}})$		$7 < P_T^{\text{jet}} < 50 \text{ GeV}$ $-1.0 < \eta_{\text{lab}}^{\text{jet}} < 2.5$	$N_{\text{jet}} \geq 1$
$\sigma_{\text{dijet}}(Q^2, \langle P_T \rangle_2)$			$N_{\text{jet}} \geq 2$ $7 < \langle P_T \rangle_2 < 50 \text{ GeV}$
$\sigma_{\text{trijet}}(Q^2, \langle P_T \rangle_3)$	$150 < Q^2 < 15\,000 \text{ GeV}^2$ $0.2 < y < 0.7$		$N_{\text{jet}} \geq 3$ $7 < \langle P_T \rangle_3 < 30 \text{ GeV}$
$\sigma_{\text{dijet}}(Q^2, \xi_2)$		$5 < P_T^{\text{jet}} < 50 \text{ GeV}$ $-1.0 < \eta_{\text{lab}}^{\text{jet}} < 2.5$ $M_{12} > 16 \text{ GeV}$	$N_{\text{jet}} \geq 2$ $0.006 < \xi_2 < 0.316$
$\sigma_{\text{trijet}}(Q^2, \xi_3)$			$N_{\text{jet}} \geq 3$ $0.01 < \xi_3 < 0.50$

The paper is at arXiv:1406.4709 since yesterday.

Further details on this analysis can be found in the theses by R. Kogler and D. Britzger
[\(http://www-h1.desy.de/publications/theses_list.html\).](http://www-h1.desy.de/publications/theses_list.html)

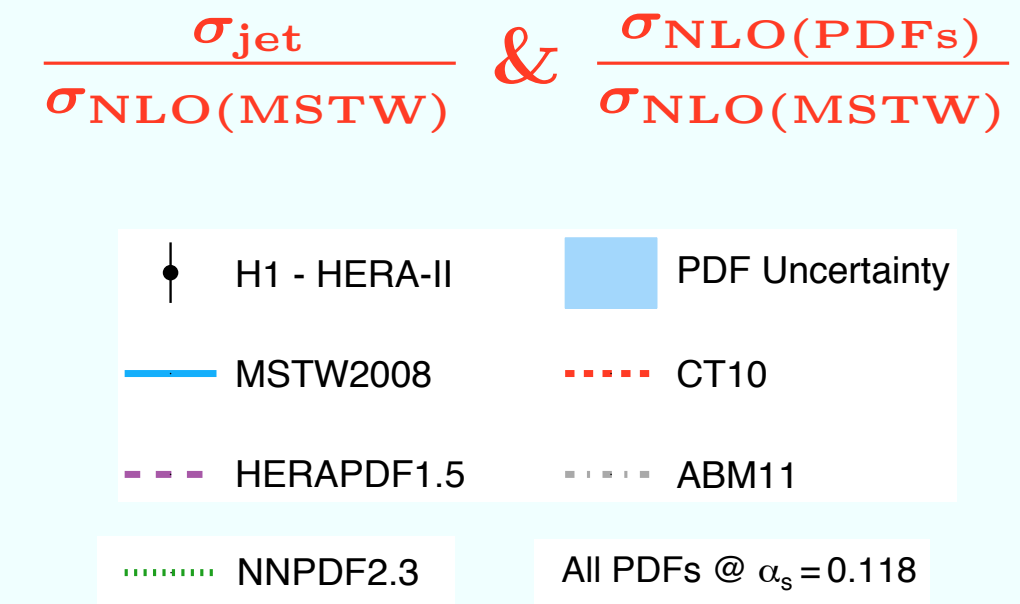
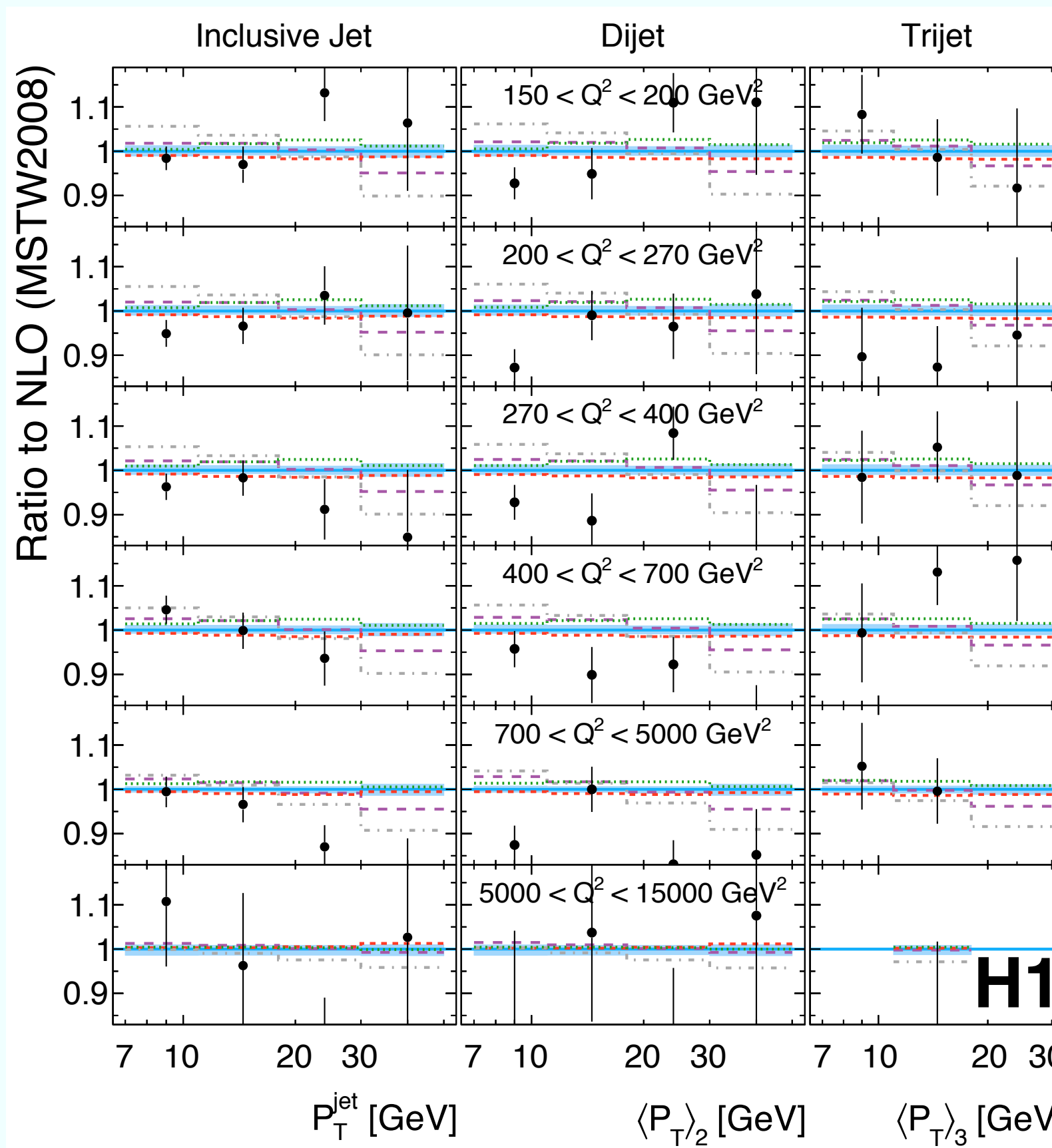
Incl. jet, dijet & trijet cross sections

$\sigma_{\text{jet}} / \sigma_{\text{NLO}}$



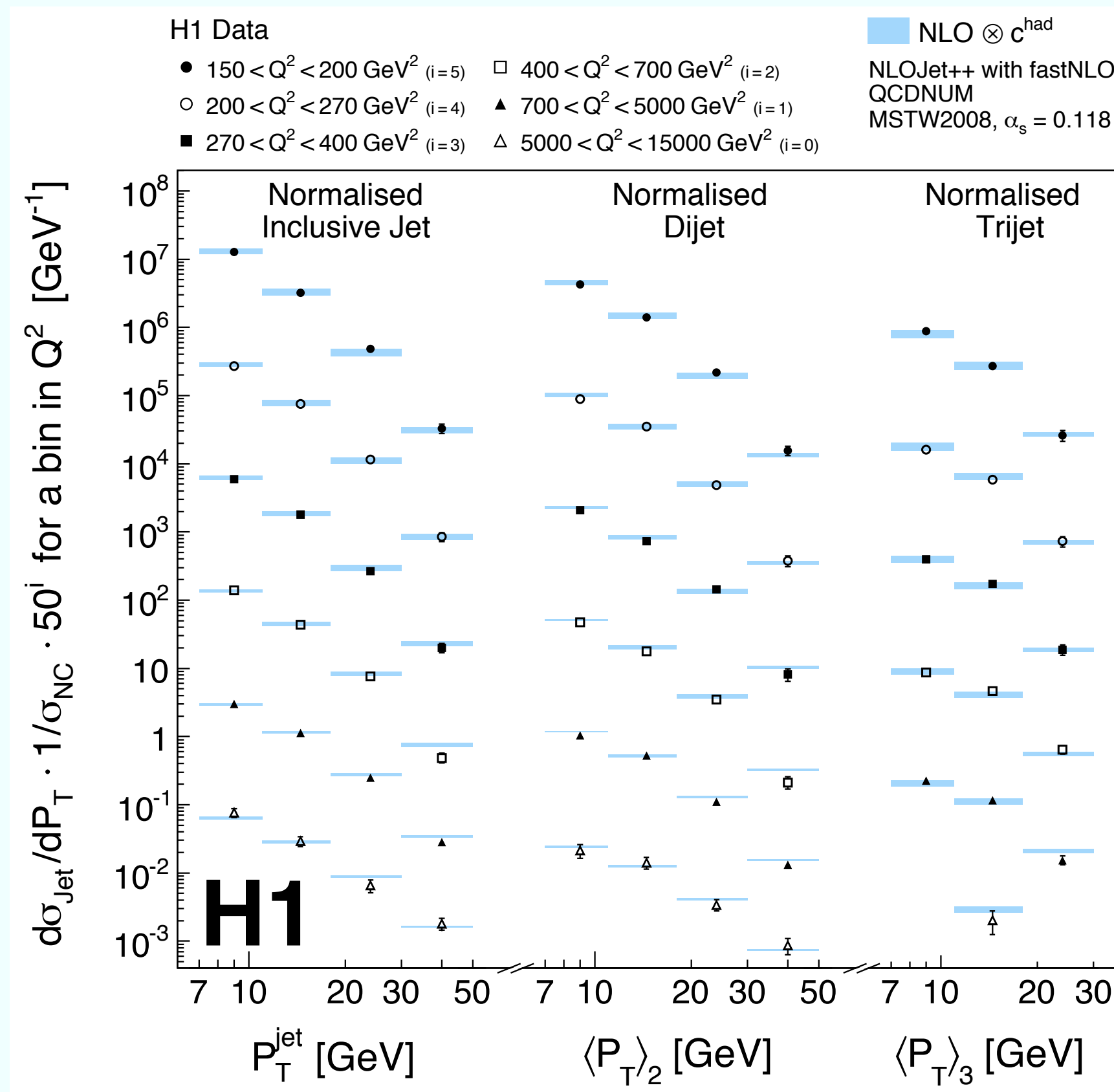
NLO in good agreement with
data within uncertainties

Comparison to NLO using different PDFs

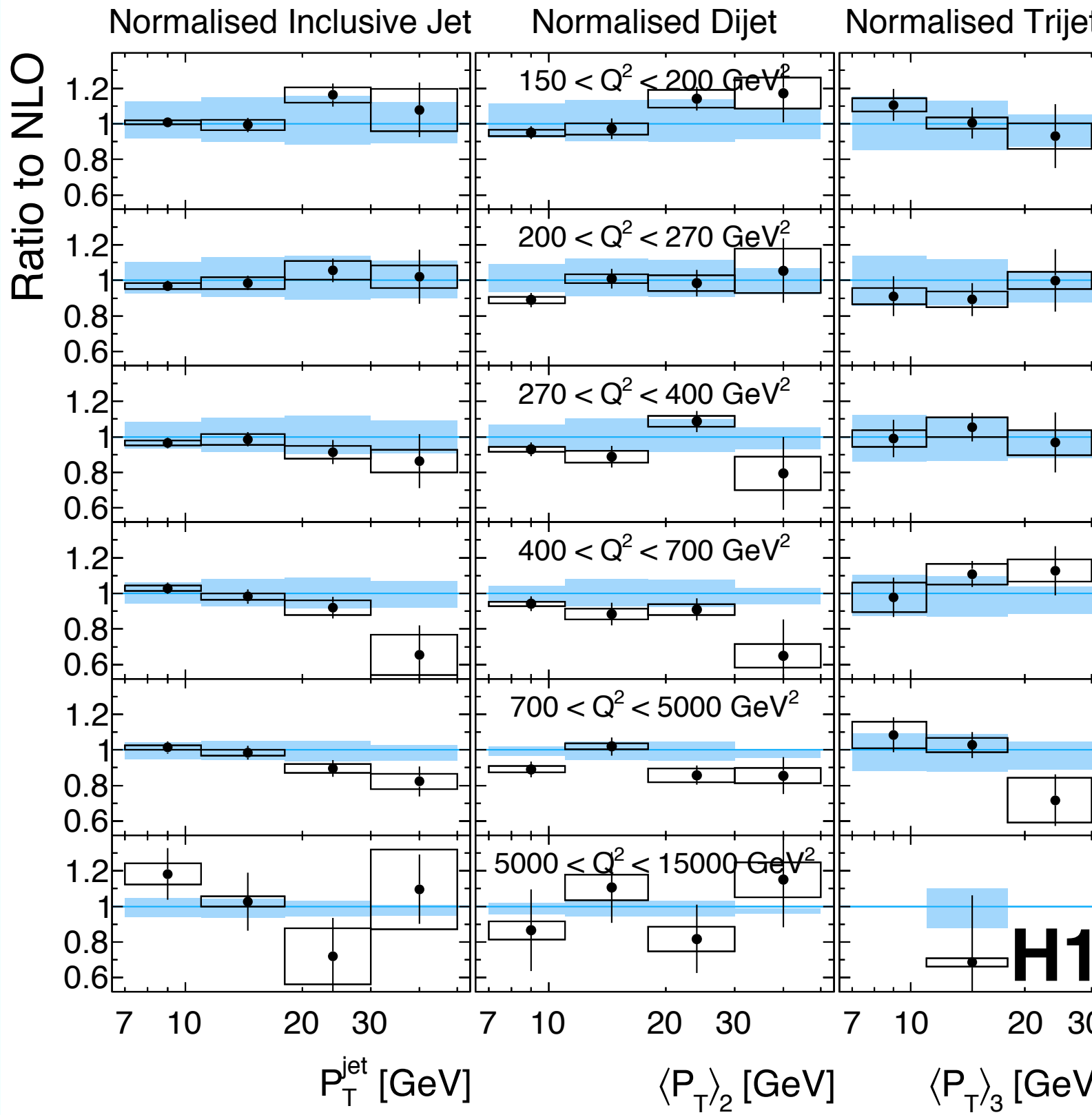


Only small differences are observed between the different PDF sets:
 CT10 about 1-2% below MSTW, NNPDF about 2% above, HERAPDF 2% above at low PT, but 5% below at the highest PT
 ABM11 shows larger differences

Norm. incl. jet, dijet & trijet cs.



Ratio: $\sigma_{\text{jet}}^{\text{norm}} / \sigma_{\text{NLO}}^{\text{norm}}$



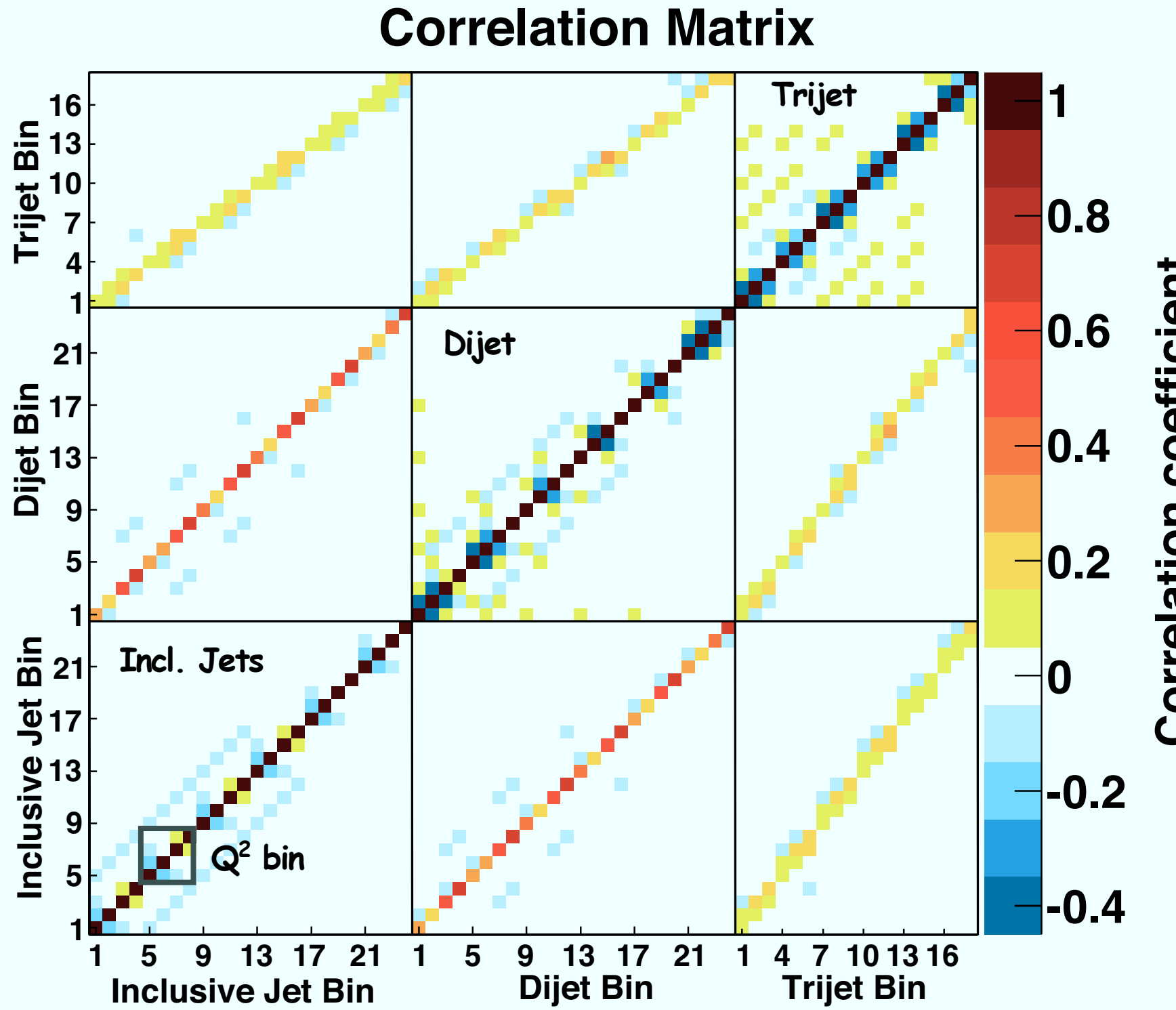
● H1 Data
□ Sys. Uncertainty
■ $\text{NLO} \otimes c^{\text{had}}$
 NLOJet++ with fastNLO, QCDNUM
 MSTW2008, $\alpha_s = 0.118$

theory uncertainty from scale variation > exp. uncertainty

exp. uncertainty dominated by stat., model and jet energy scale uncertainty

normalized dijet cross sections below the NLO predictions for many data points

Correlation matrix



correlations down to -0.5 between adjacent bins in $P_{T,jet}$ in a given Q^2 bin (due to only moderate resolution in $P_{T,jet}$)

about -0.1 in neighboring Q^2 bins (excellent resol. in Q^2)

sizeable positive corr. between incl. jet and dijet in the same Q^2 bin and similar $P_{T,jet}$

smaller pos. corr. between trijets and the other two samples (smaller stat. overlap)

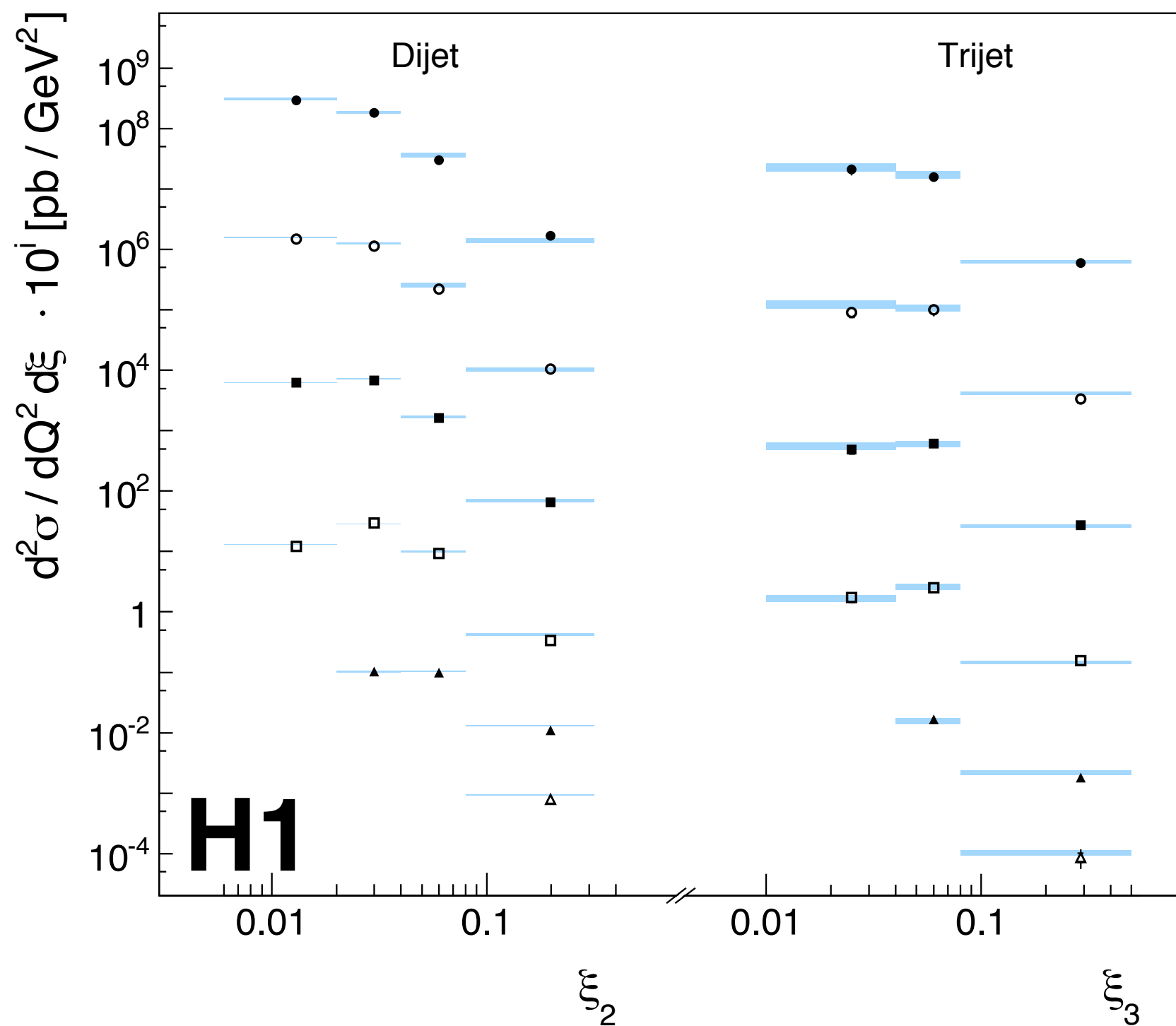
Dijet & trijet vs. Q^2 & ξ

H1 Data

- $150 < Q^2 < 200 \text{ GeV}^2$ ($i=7$) □ $400 < Q^2 < 700 \text{ GeV}^2$ ($i=1$)
- $200 < Q^2 < 270 \text{ GeV}^2$ ($i=5$) ▲ $700 < Q^2 < 5000 \text{ GeV}^2$ ($i=0$)
- $270 < Q^2 < 400 \text{ GeV}^2$ ($i=3$) △ $5000 < Q^2 < 15000 \text{ GeV}^2$ ($i=0$)

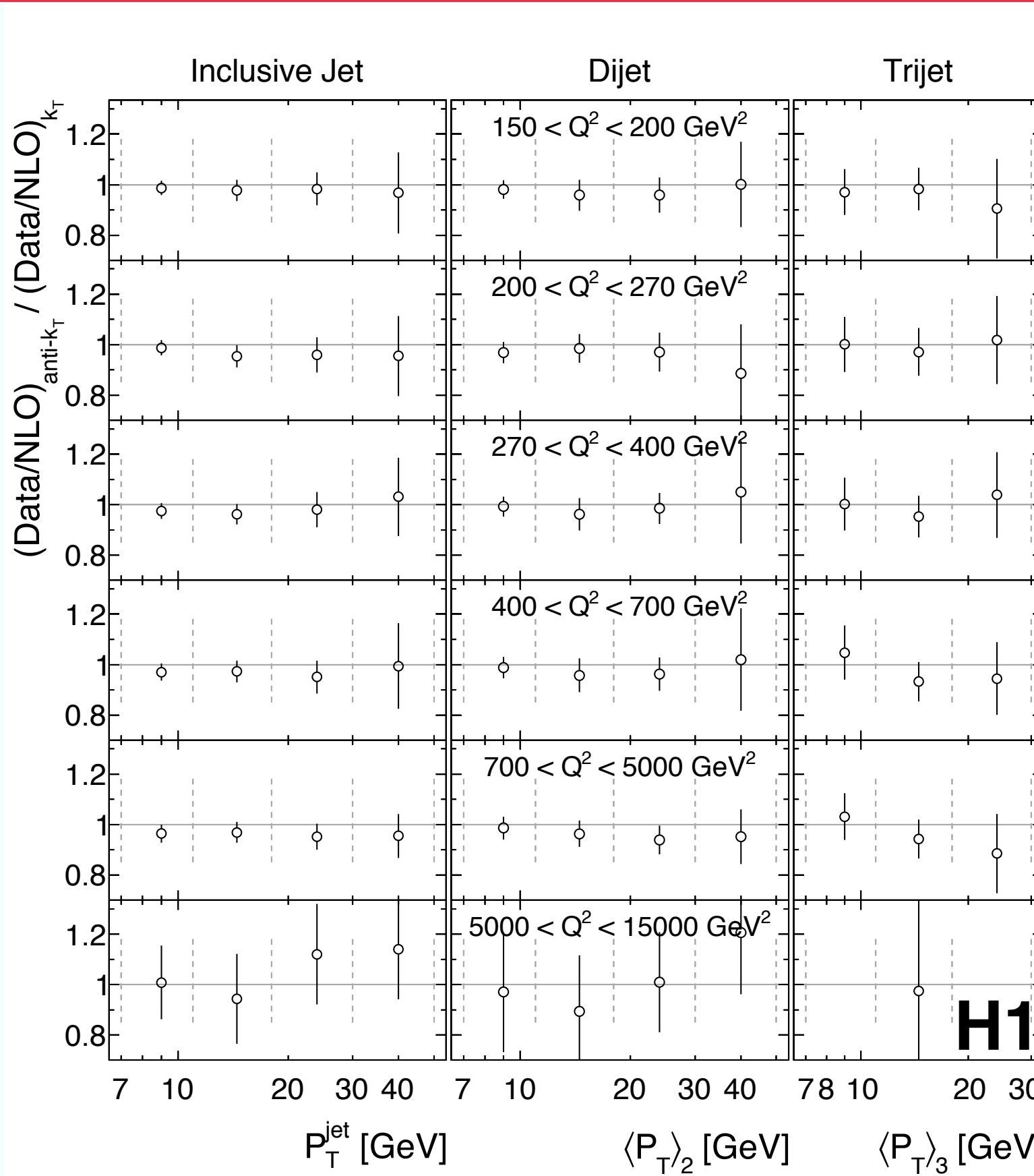
NLO $\otimes c^{\text{had}} \otimes c^{\text{ew}}$

NLOJet++ with fastNLO
MSTW2008, $\alpha_s = 0.118$



here, "low- x " is:
 $6 \times 10^{-3} < \xi < 0.5$

$$(\sigma^{\text{anti-}k_T} / \sigma^{\text{anti-}k_T}_{\text{NLO}}) / (\sigma^{k_T} / \sigma^{k_T}_{\text{NLO}})$$



Ratio of anti- k_T and k_T cross sections to corresponding NLO predictions is consistent with 1 for incl. jets and dijets

For trijets it tends to be less than 1

Extraction of $\alpha_s(M_Z)$

Fit NLO QCD calculations with $\alpha_s(M_Z)$ as free parameter to absolute and norm. incl. jet, dijet & trijet cross sections (individually and simultaneously):

$$\chi^2(\alpha_s(M_Z), \varepsilon_k) = \vec{p}^T V^{-1} \vec{p} + \sum_k^{N_{\text{sys}}} \varepsilon_k^2 \quad p_i = \log m_i - \log t_i - \sum_k^{N_{\text{sys}}} E_{i,k}$$

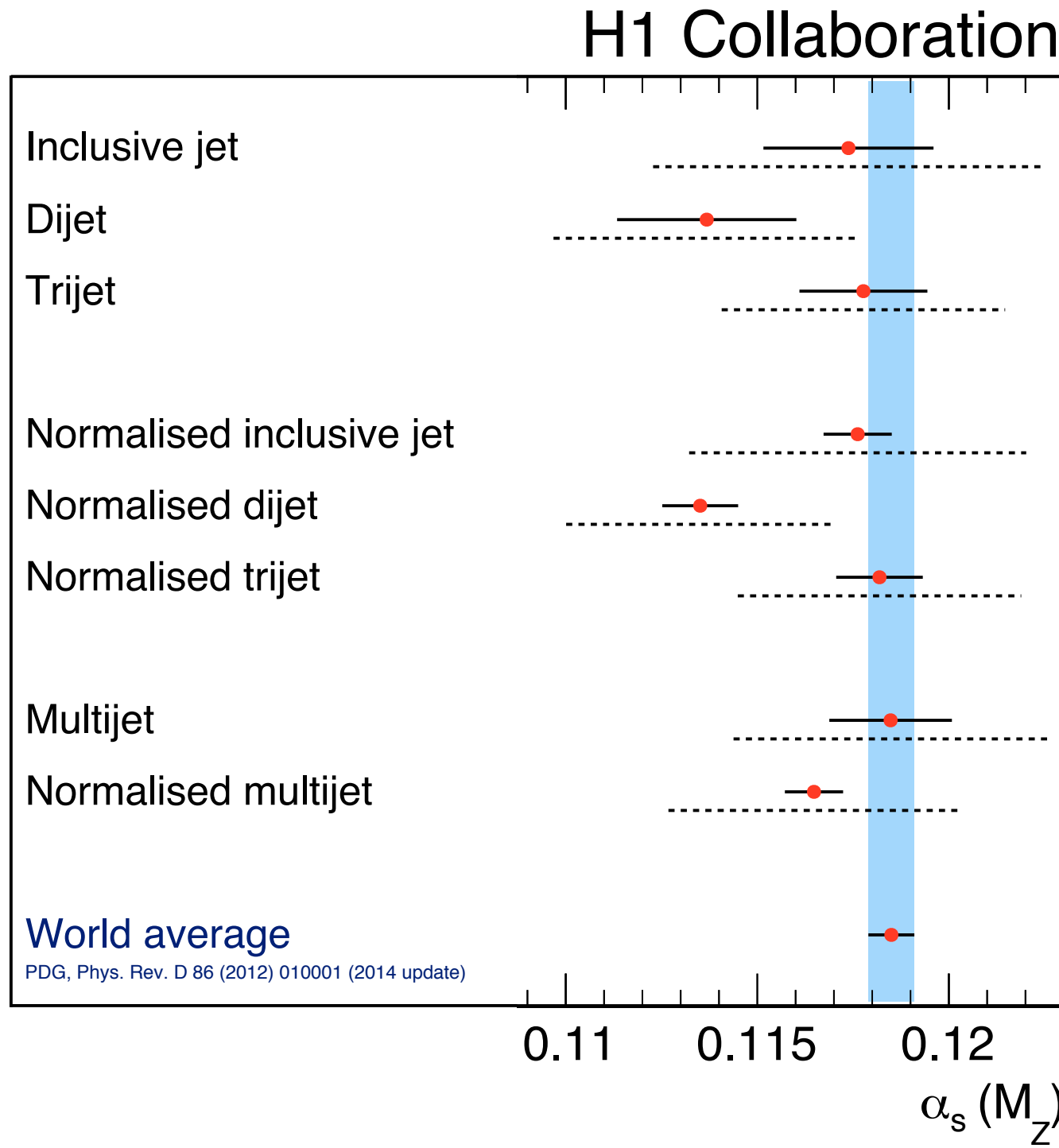
The m_i refer to the unfolded measurements and $t_i(\alpha_s(M_Z))$ to the theory prediction. This ansatz assumes log-normal distributed m_i with $E_{i,k}$ defined by:

$$E_{i,k} = \sqrt{f_k^C} \left(\frac{\delta_{m,i}^{k,+} - \delta_{m,i}^{k,-}}{2} \varepsilon_k + \frac{\delta_{m,i}^{k,+} + \delta_{m,i}^{k,-}}{2} \varepsilon_k^2 \right)$$

The covariance matrix V consists of the relative stat. uncertainties, including correlations between the data points and the uncorrelated part of the syst. uncertainties.

The theory uncertainties are determined for each source separately using linear error propagation.

Summary of $\alpha_s(M_Z)$ from this analysis



consistent results within total uncertainties and with world average

tension between dijet and other results within exp. uncertainties

most precise result when using norm. multijet cross sections

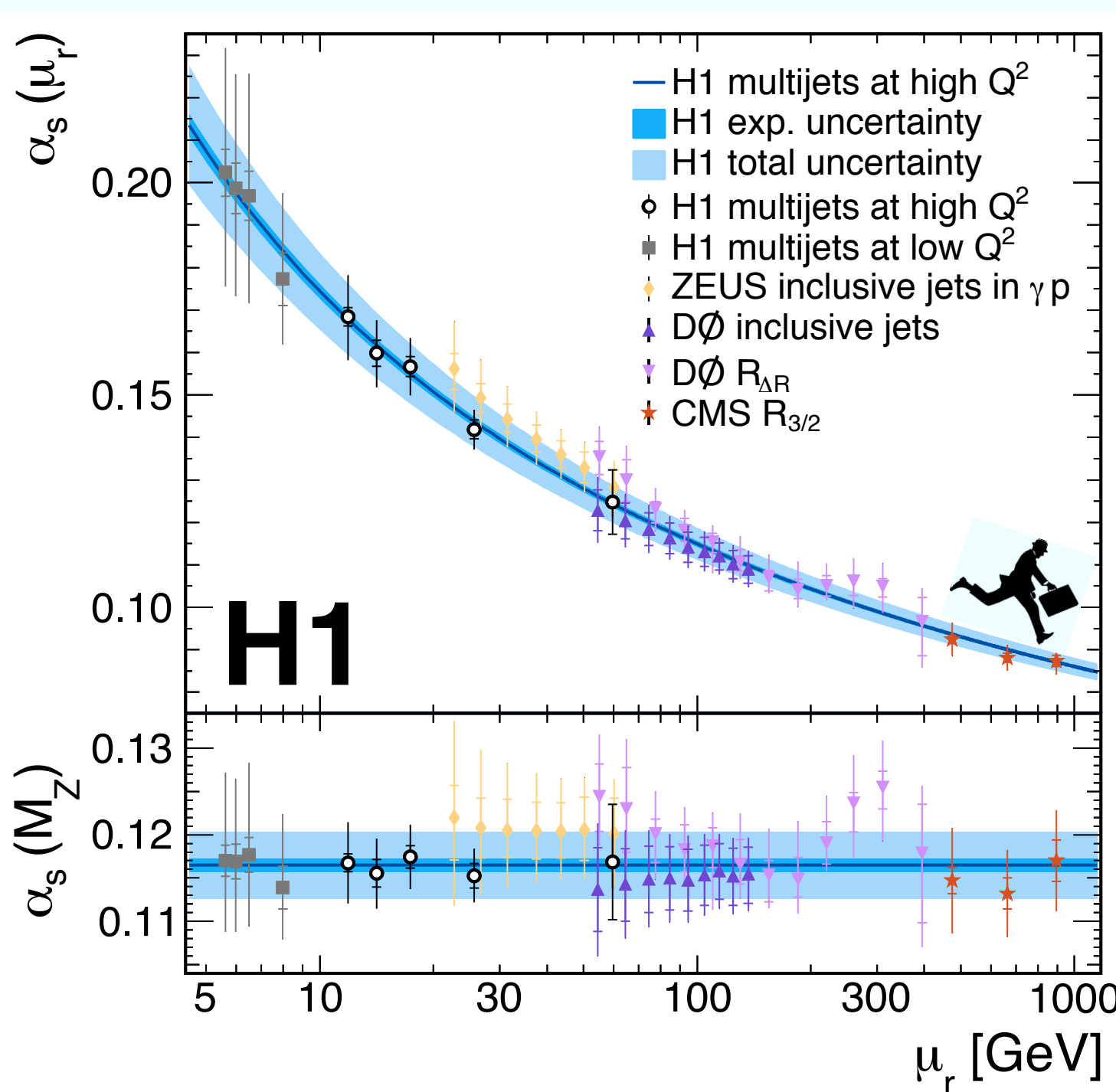
need NNLO calculations to match the superior exp. precision (0.7%)

$$\alpha_s(M_Z)|_{k_T} = 0.1165 \text{ (8)}_{\text{exp}} \text{ (5)}_{\text{PDF}} \text{ (7)}_{\text{PDFset}} \text{ (3)}_{\text{PDF}(\alpha_s)} \text{ (8)}_{\text{had}} \text{ (36)}_{\mu_r} \text{ (5)}_{\mu_f}$$

= 0.1165 (8)_{exp} (38)_{pdf, theo}

Running of $\alpha_s(\mu_r)$

$\alpha_s(\mu_r)$ from 5 fits using the norm. multijet cross sections, each fit based on a set of measurements with comparable values of μ_r



the $\alpha_s(M_Z)$ -values are found to be consistent and independent of μ_r

they agree with H1 data at lower scales and with other data at higher scales

the prediction for the running, using the RGE and

$$\alpha_s(M_Z) = 0.1165 \text{ (8)}_{\text{exp}} \text{ (38)}_{\text{pdf, theo}}$$

agrees well with the measurements

Summary

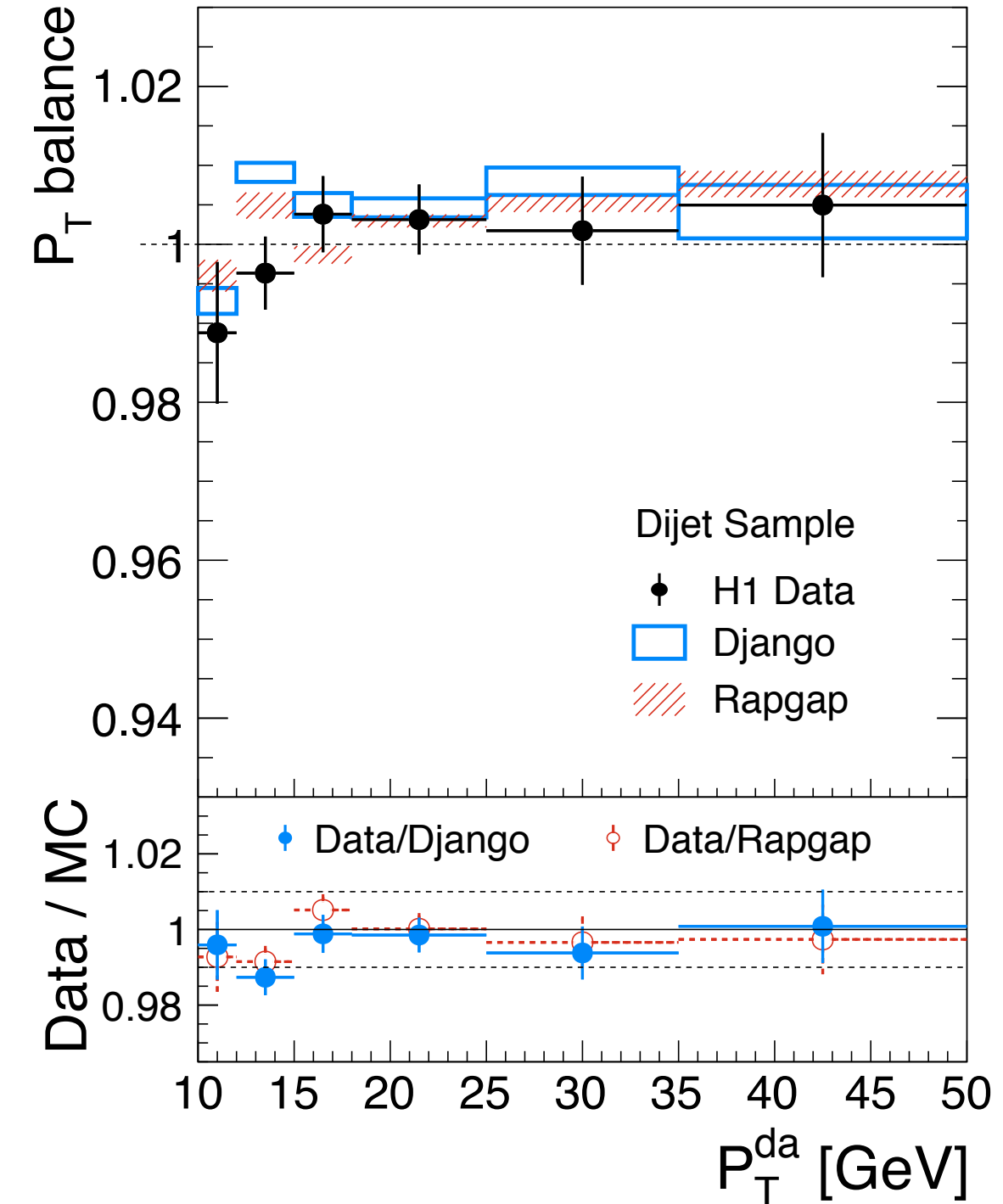
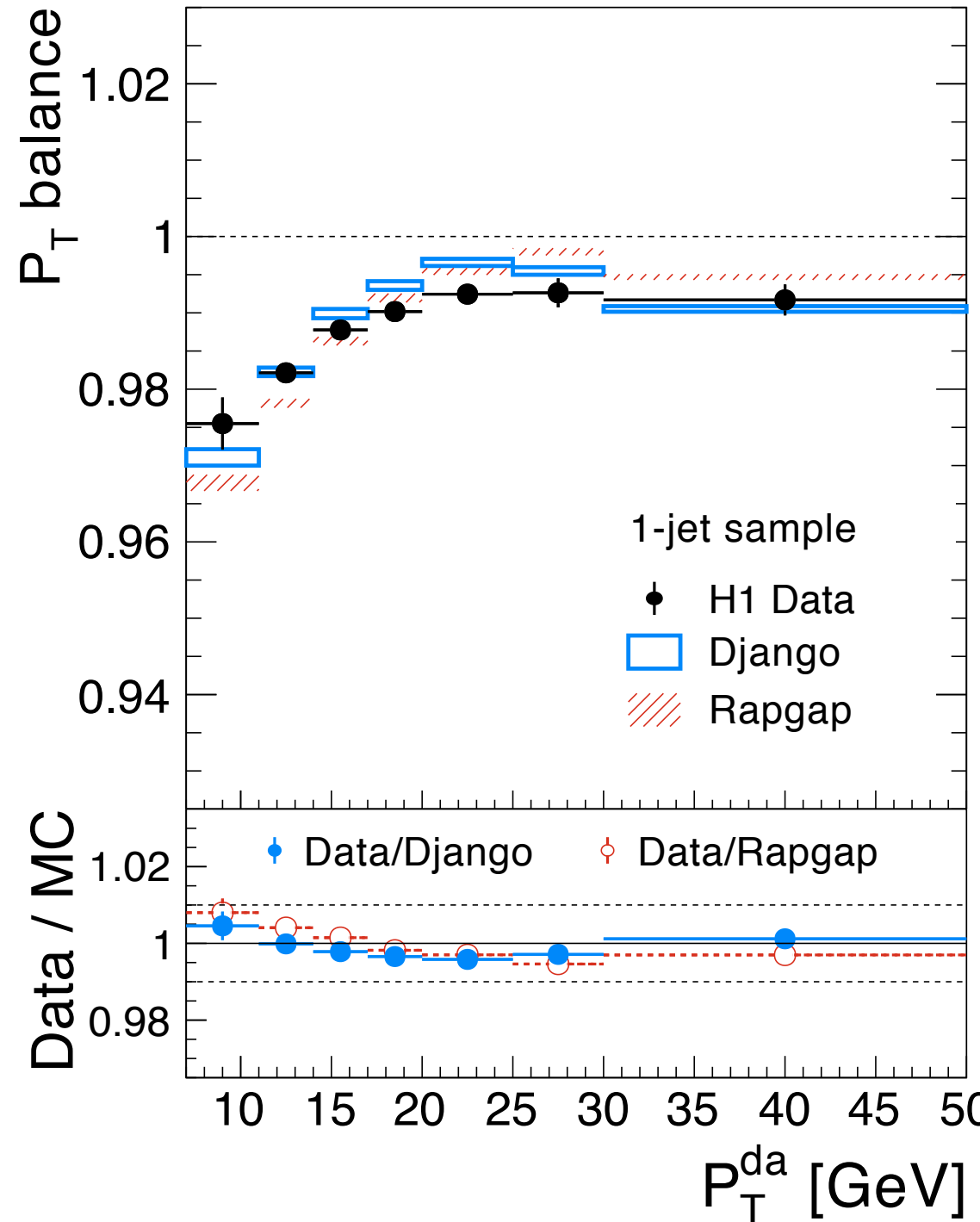
- Final precision results by H1 on absolute and normalized, k_T and anti- k_T , multijet cross sections in DIS using:
 - various improvements to yield an hadronic energy scale uncertainty of 1%
 - regularized simultaneous unfolding of NC DIS data and the jet data yield stable results, good control of migrations, and the determination of correlations between the measurements.
- In general, the precision of the measurement is better than that of the NLO prediction.
- Consistent values of $\alpha_s(M_Z)$ are obtained from the individual jet cross sections, but there is tension between the $\alpha_s(M_Z)$ -value from dijets compared to the similar values from incl. jets and trijets, which could be a sign of different higher order corrections.
- Most precise $\alpha_s(M_Z)$ is extracted from fit to the normalized multijet cross sections, yielding: $\alpha_s(M_Z)|_{k_T} = 0.1165 \text{ (8)}_{\text{exp}} \text{ (38)}_{\text{pdf, theo}}$
- The running of $\alpha_s(\mu_r)$ is consistent with the RGE and with results from other jet data.
- NNLO calculations are needed to match the exp. precision

A photograph of a traditional Japanese garden. In the foreground, there is a low, curved stone lantern with a thatched roof. To its left is a large, dark, craggy rock. Behind the lantern is a wide, light-colored gravel path. Several large, smooth stones are scattered along the path. In the background, there is a dense forest of green trees and bushes. The overall atmosphere is peaceful and serene.

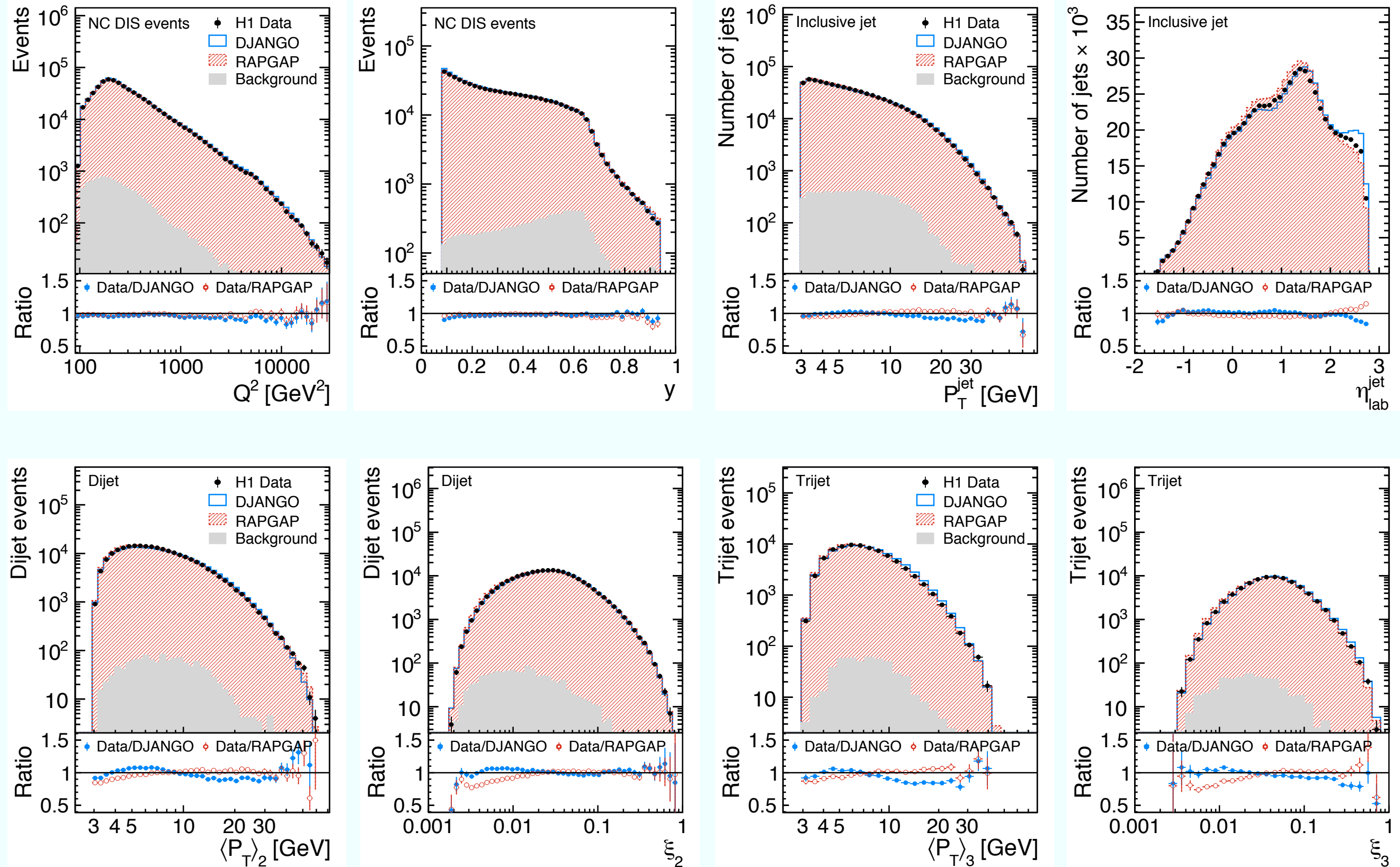
ありがとうございます

Additional material

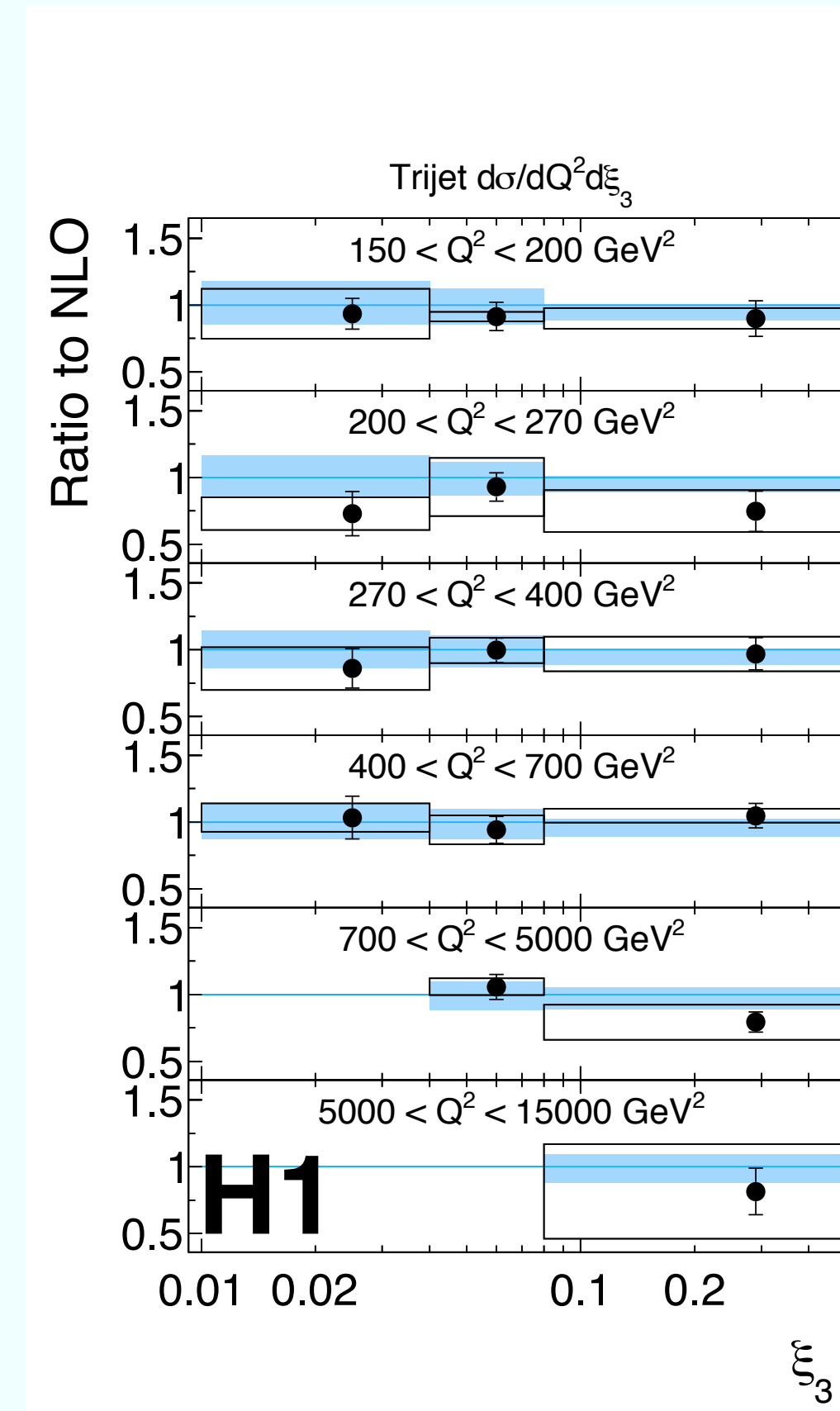
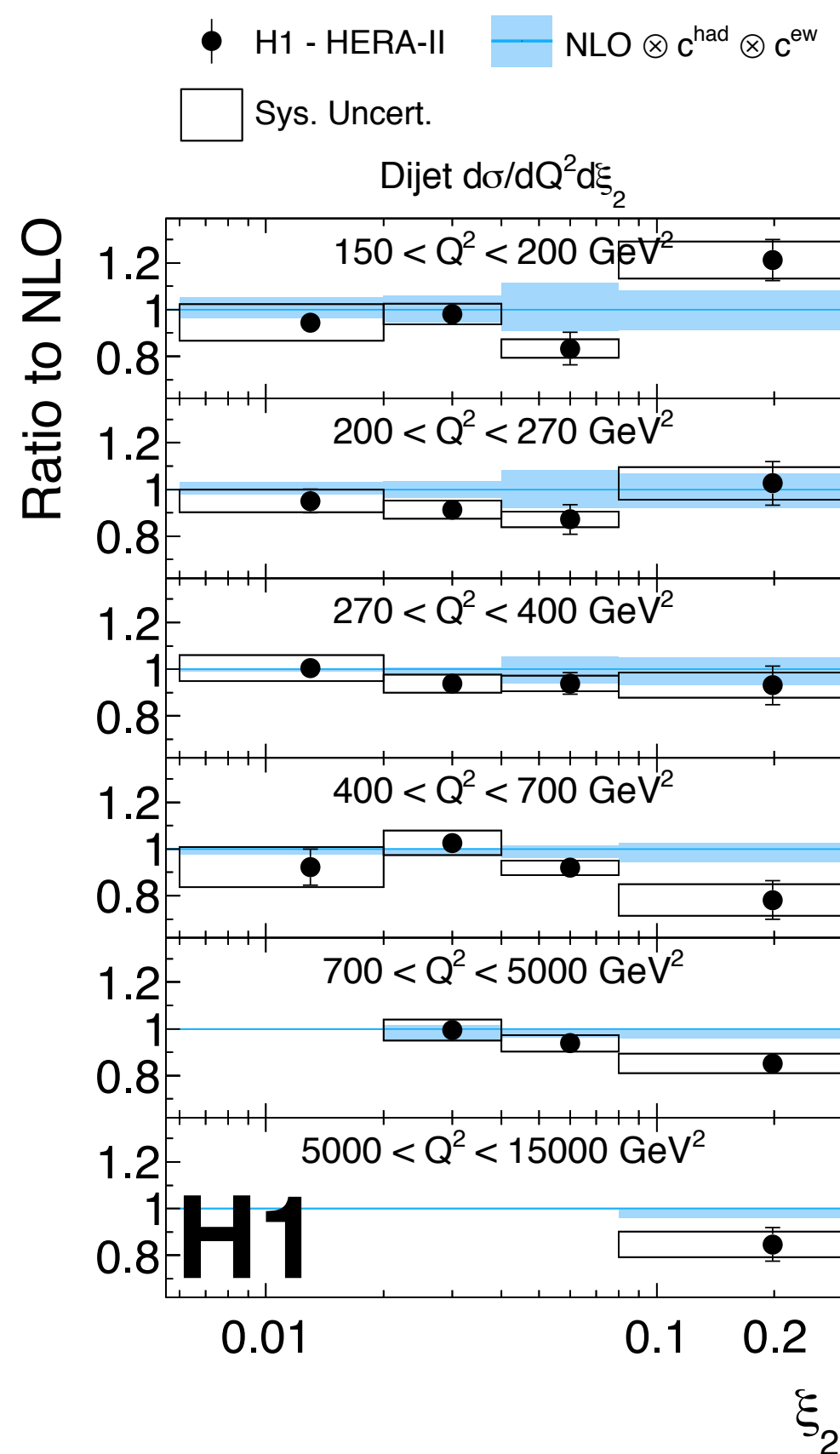
Calibration plots



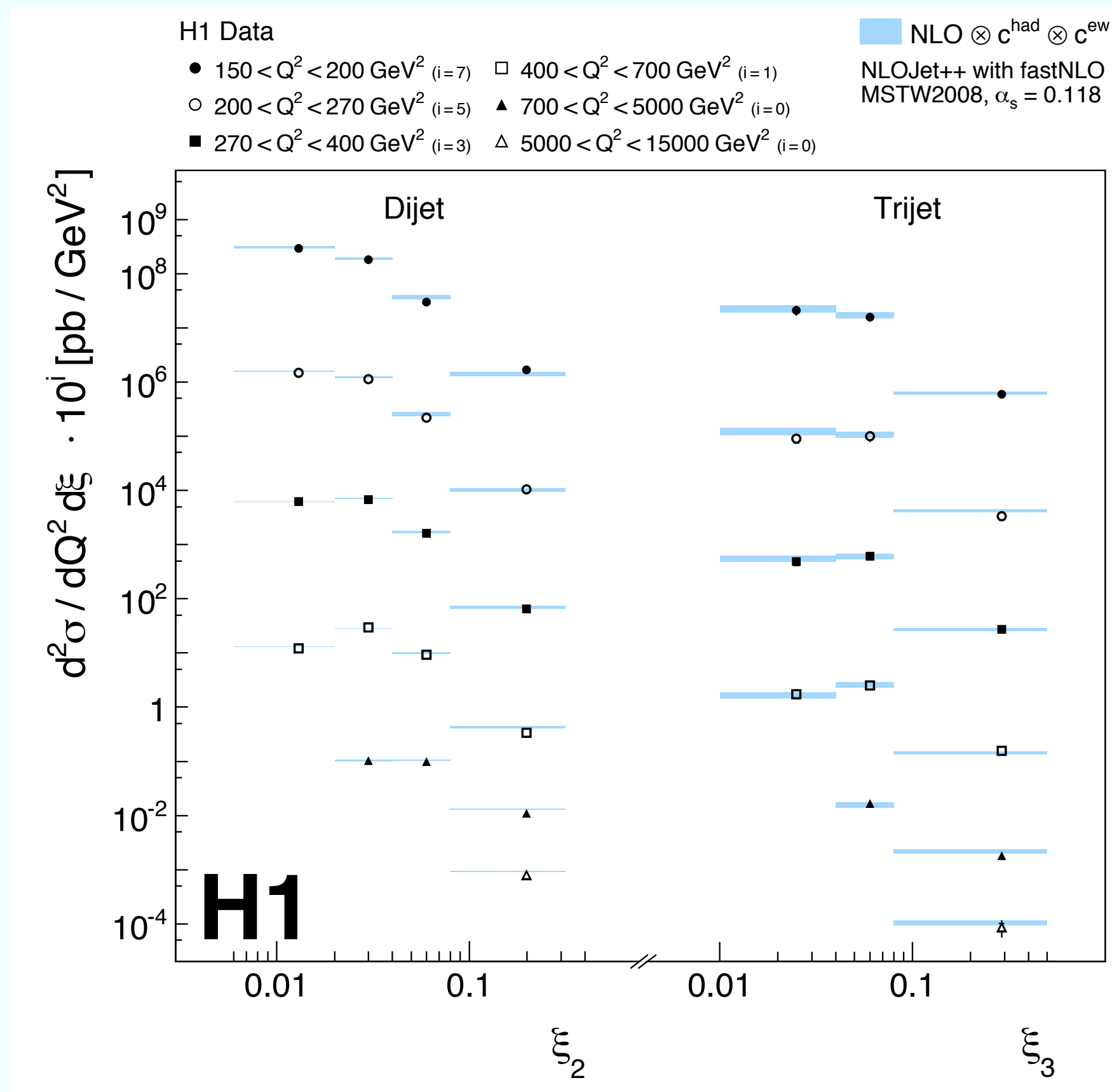
Control plots



Ratio: $\sigma_{\text{dijet}} (\sigma_{\text{trijet}}) / \sigma_{\text{NLO}}$



Norm. dijet & trijet vs. Q^2 & ξ



Break-down of syst. uncertainties

as used in fit of $\alpha_s(M_Z)$

Source of uncertainties k	Correlated fraction f^C	Uncorrelated fraction f^U	Uncorrelated between Q^2 bins
Jet energy scale δ^{JES}	0.5	0.5	
Rem. cluster energy scale δ^{RCES}	0.5	0.5	
LAr Noise δ^{LArNoise}	1	0	
Electron energy $\delta^{E'_e}$	1	0	✓
Electron polar angle δ^{θ_e}	1	0	✓
Electron ID $\delta^{\text{ID}(e)}$	1	0	✓
Normalisation δ^{Norm}	1	0	
Model δ^{Model}	0.25	0.75	✓

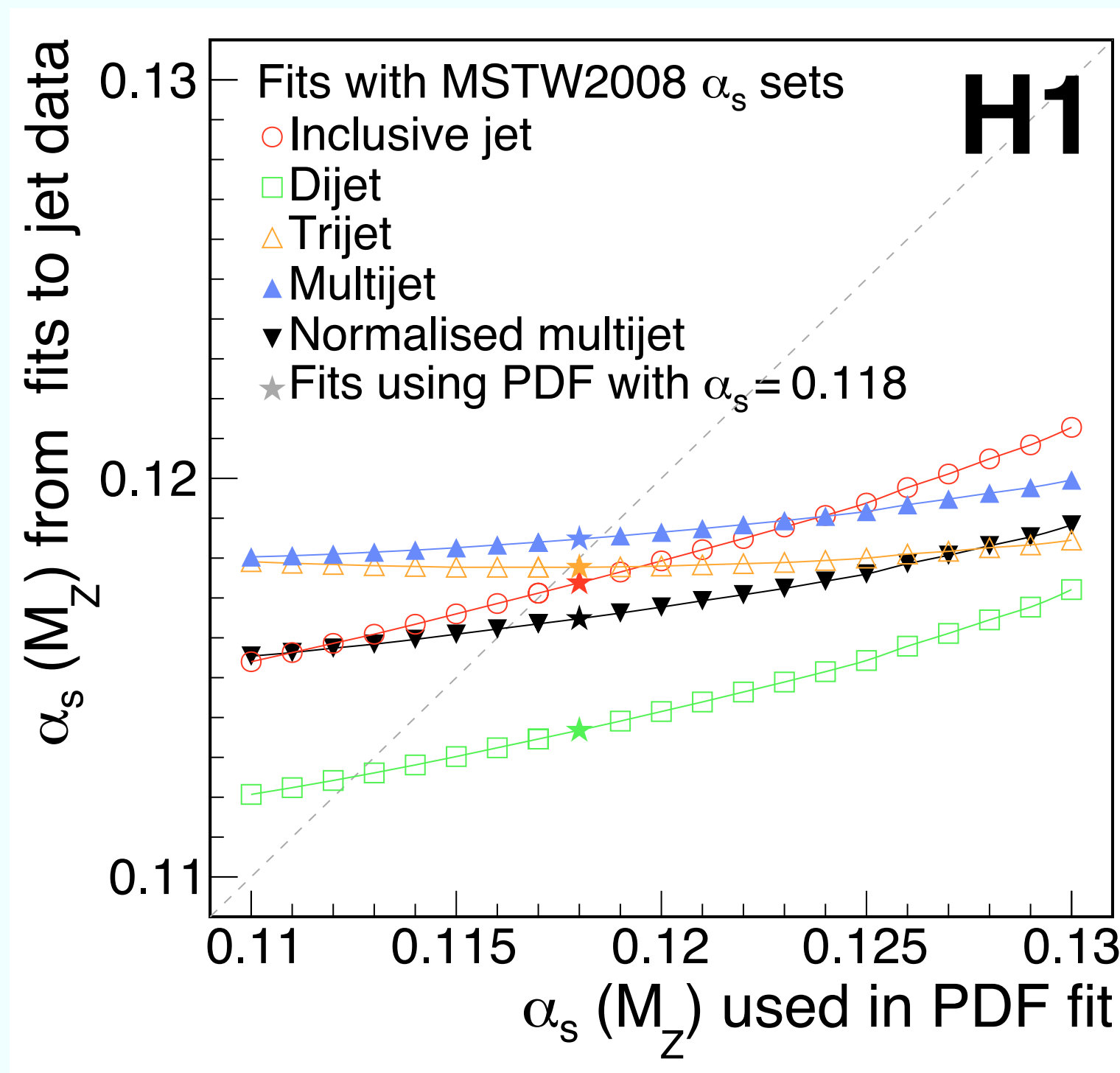
Experimental uncertainties on $\alpha_s(M_Z)$

dominant uncertainties only

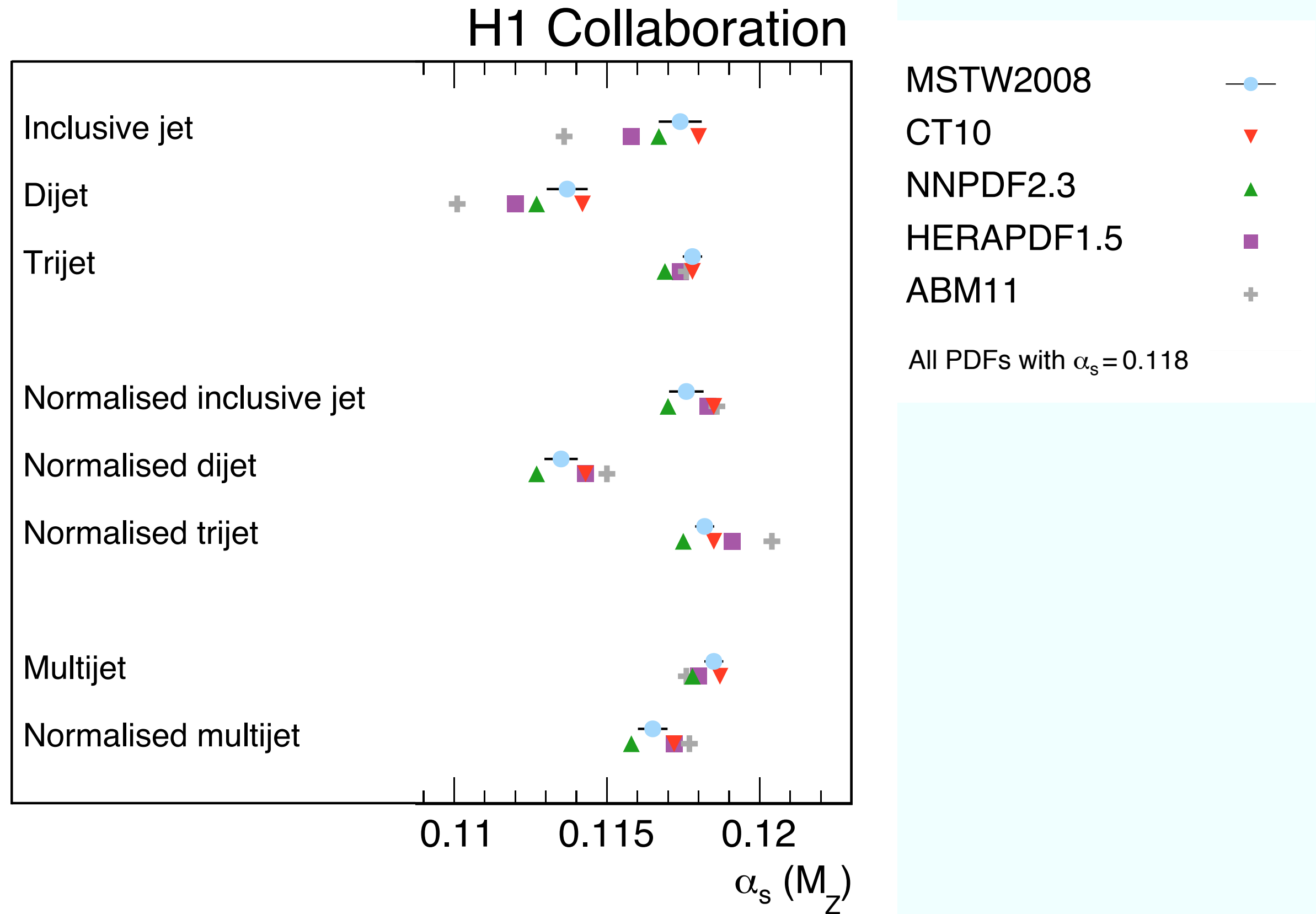
Experimental uncertainties on $\alpha_s \times 10^4$

Measurement	$\Delta_{\alpha_s}^{\text{exp}}$	$\Delta_{\alpha_s}^{\text{Norm}}$	$\Delta_{\alpha_s}^{\text{RCES}}$	$\Delta_{\alpha_s}^{\text{JES}}$	$\Delta_{\alpha_s}^{\text{Model}}$
σ_{jet}	22.2	18.5	4.8	5.5	4.5
σ_{dijet}	23.4	19.4	4.4	4.3	6.4
σ_{trijet}	16.7	11.2	5.4	4.3	4.6
$\frac{\sigma_{\text{jet}}}{\sigma_{\text{NC}}}$	8.9	–	1.7	4.4	2.2
$\frac{\sigma_{\text{dijet}}}{\sigma_{\text{NC}}}$	9.9	–	1.6	3.3	3.6
$\frac{\sigma_{\text{trijet}}}{\sigma_{\text{NC}}}$	11.3	–	4.0	3.5	4.2
$[\sigma_{\text{jet}}, \sigma_{\text{dijet}}, \sigma_{\text{trijet}}]$	16.0	9.6	5.9	3.2	5.0
$\left[\frac{\sigma_{\text{jet}}}{\sigma_{\text{NC}}}, \frac{\sigma_{\text{dijet}}}{\sigma_{\text{NC}}}, \frac{\sigma_{\text{trijet}}}{\sigma_{\text{NC}}} \right]$	7.6	–	2.4	2.8	1.8

$\alpha_s(M_Z)$ from jet fit vs. $\alpha_s(M_Z)$ of PDF



$\alpha_s(M_Z)$ obtained using different PDFs



Summary of values of $\alpha_s(M_Z)$ and uncertainties

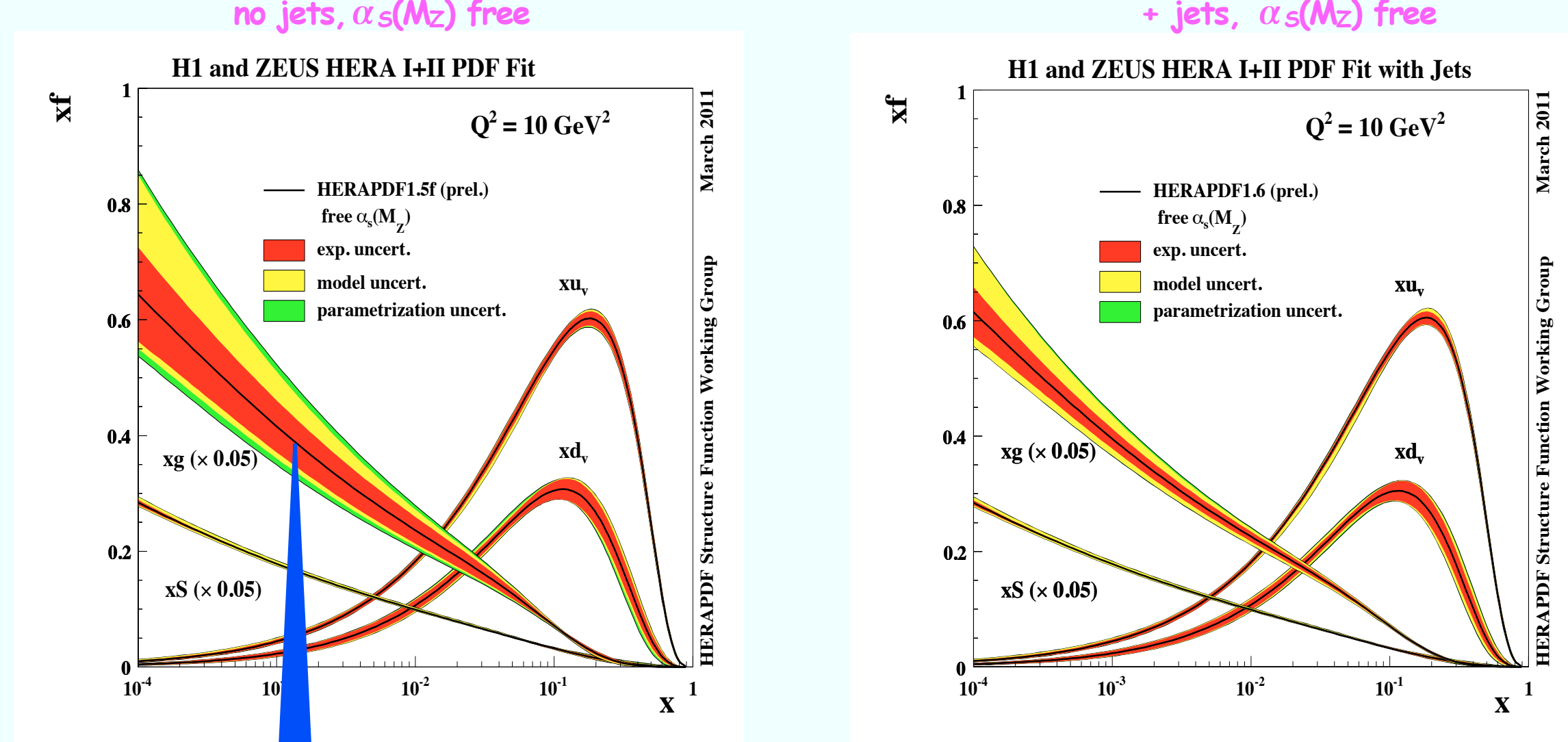
Cross sections	$\alpha_s(M_Z) _{k_T}$	$\alpha_s(M_Z) _{\text{anti}-k_T}$	Theoretical uncertainties
σ_{jet}	0.1174(22) _{exp}	0.1175(22) _{exp}	(7) _{PDF} (7) _{PDFset} (5) _{PDF(α_s)} (10) _{had} (48) _{μ_r} (6) _{μ_f}
σ_{dijet}	0.1137(23) _{exp}	0.1152(23) _{exp}	(7) _{PDF} (7) _{PDFset} (5) _{PDF(α_s)} (7) _{had} (37) _{μ_r} (6) _{μ_f}
σ_{trijet}	0.1178(17) _{exp}	0.1174(18) _{exp}	(3) _{PDF} (5) _{PDFset} (0) _{PDF(α_s)} (11) _{had} (34) _{μ_r} (3) _{μ_f}
$\frac{\sigma_{\text{jet}}}{\sigma_{\text{NC}}}$	0.1176(9) _{exp}	0.1172(8) _{exp}	(6) _{PDF} (7) _{PDFset} (4) _{PDF(α_s)} (8) _{had} (41) _{μ_r} (6) _{μ_f}
$\frac{\sigma_{\text{dijet}}}{\sigma_{\text{NC}}}$	0.1135(10) _{exp}	0.1147(9) _{exp}	(5) _{PDF} (8) _{PDFset} (3) _{PDF(α_s)} (6) _{had} (32) _{μ_r} (6) _{μ_f}
$\frac{\sigma_{\text{trijet}}}{\sigma_{\text{NC}}}$	0.1182(11) _{exp}	0.1177(12) _{exp}	(3) _{PDF} (5) _{PDFset} (0) _{PDF(α_s)} (11) _{had} (34) _{μ_r} (3) _{μ_f}
$[\sigma_{\text{jet}}, \sigma_{\text{dijet}}, \sigma_{\text{trijet}}]$	0.1185(16) _{exp}	0.1181(17) _{exp}	(3) _{PDF} (4) _{PDFset} (2) _{PDF(α_s)} (13) _{had} (38) _{μ_r} (3) _{μ_f}
$\left[\frac{\sigma_{\text{jet}}}{\sigma_{\text{NC}}}, \frac{\sigma_{\text{dijet}}}{\sigma_{\text{NC}}}, \frac{\sigma_{\text{trijet}}}{\sigma_{\text{NC}}} \right]$	0.1165(8) _{exp}	0.1165(7) _{exp}	(5) _{PDF} (7) _{PDFset} (3) _{PDF(α_s)} (8) _{had} (36) _{μ_r} (5) _{μ_f}

Inclusive jets in DIS in PDF fits

Inclusive jets from H1 and ZEUS in bins of Q^2 and P_T are added in the PDF fit

H1prelim-11-034
ZEUS-prel-11-001

reminder: jets are sensitive in LO to $\alpha_s \otimes g$ (BGF) and α_s (QCDC)

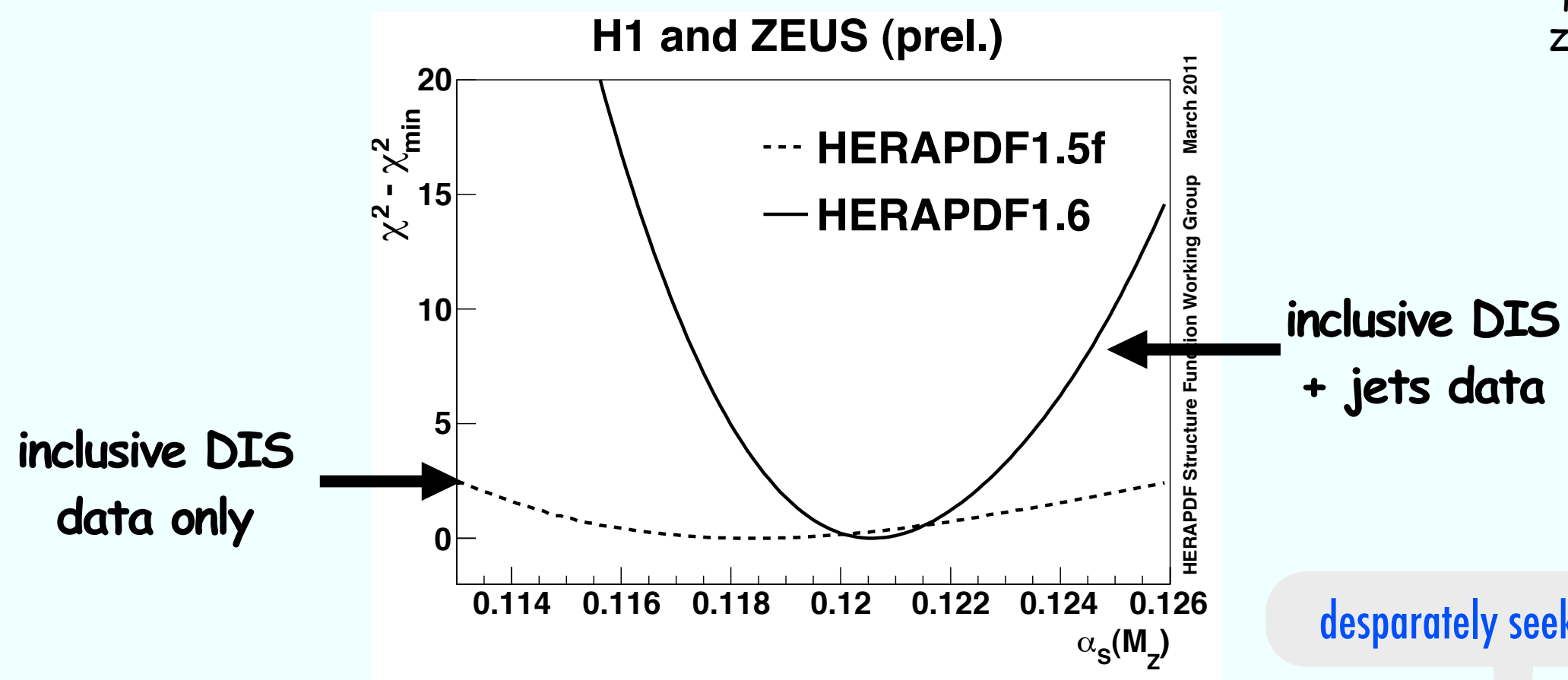


the gluon uncertainty
at low- x blows up

adding jet data dramatically decreases
the low- x gluon uncertainty, not only
the experimental but also the model and
parameterization uncertainties

$\alpha_s(M_Z)$ from incl. DIS & jets in DIS

H1prelim-11-034
ZEUS-prel-11-001



→ adding jet data successfully reduces the correlation between α_s and the gluon

$$\alpha_s(M_Z) = 0.1202 \pm 0.0019(\text{exp}/\text{model}/\text{param}/\text{hadronization})^{+0.0045}_{-0.0036}(\text{scale})$$

1.6% uncertainty + 3-3.7% scale unc.

scale uncertainty from variation of renormalization & factorization scale by a factor of $\frac{1}{2}$ and 2